The Second International Conference on Saltwater Intrusion and Coastal Aquifers —
Monitoring, Modeling and Management. Merida, Yucatan, Mexico, March 30-April 2, 2003

The Impact of Future Possible Sea Level Rise on Saltwater Intrusion in Coastal Aquifers and the Effect of Some Protective Measures for Coastal Environment

K.Fujinawa [1]

[1] Shinshu Univeristy, Japan

ABSTRACT

According to IPCC, global average seal level is projected to rise by 9 to 88 cm between 1990 and 2100. The sea level rise can not only enhance saltwater intrusion into coastal aquifers but also force us to keep draining induced inland water in low land areas below sea level such as the mega cities in Japan subsided due to the past excessive withdrawal of groundwater. The impacts of sea level rise were studied by laboratory experiments and the effect of barrier walls for reducing saltwater intrusion was investigated. A variable density flow model which couples a fluid flow equation with a mass transport equation was applied to solve the problem numerically by using a finite element method for fluid flow and a characteristic finite element method for mass transport. The numerical results were compared with some experimental results and the accuracy of the numerical scheme was examined.

INTRODUCTION

862 km^2 of the land in Japan, inhabited by people of 2 million, lies below high-tide sea level. In low lying delta of Tokyo, suffering from historical land subsidence, outer dykes of 4.6-8.0 m high and inner dykes of 3.0 m high were built to protect inland area of 124 km^2 from storm surges and excess water is kept drained to control inland surface water level.

According to the third assessment report released in January, 2001 by the Intergovernmental Panel on Climate Change [2001], global average sea level rise is projected to rise by 9 to 88 cm between 1990 and 2100. The impacts of sea level rise will be complex both physically and socio-economically. Sea water intrusion into fresh water aquifers in deltaic areas is one of the major impacts of sea level rise. Laboratory experiments with flat and inclined surfaces were conducted to investigate the influence of sea level rise on salt water intrusion together with the effect of barrier walls and drainage of seeped-out inland water for preventing inundation. Results of the experiments were also used to validate a numerical model for variable-density fluid flow coupled with mass transport.

EXPERIMENTS

Fig.1a shows experimental apparatus which was packed with glass beads of mean diameter 0.6 mm. Infiltration zone with flat surface has dimension of 700 mm × 400 mm × 100 mm. Fresh water is supplied from fresh water reservoir and flows in the upper zone from left to right boundary while salt water is supplied from salt water tank and intrude into the lower zone from right boundary.

Fresh water level was kept at height of 400 mm from the bottom of the apparatus on the left boundary while salt water level was raised step by step from 350 mm to 377 mm on the right boundary. Density of fresh water was 0.999 g/cm^3 and that of salt water was 1.058 g/cm^3. Experiments with barrier walls of various depth, installed 150 mm left of the right boundary, were also conducted and its effect for preventing salt water intrusion was investigated.

Fig.1b shows a set up for the second experiments having a descending surface from left to right boundary, and an impervious dike for preventing over flow of salt water was installed at the right boundary with the lower edge at height of 250 mm from the bottom of the apparatus. The density of fresh water was 0.999 g/cm^3 and that of salt water was 1.029 g/cm^3 for these experiments.

In every experiments, salt water was colored by uranine for pictures taken by a digital camera. Fluid samples of 5 ml were collected from sampling holes of back panel of the apparatus to investigate concentration distribution of salt water by measuring electric conductivity. Uranine was also used as tracer to draw stream lines by injecting from tracer injection holes. Average porosity of the glass-beads media was 0.364.

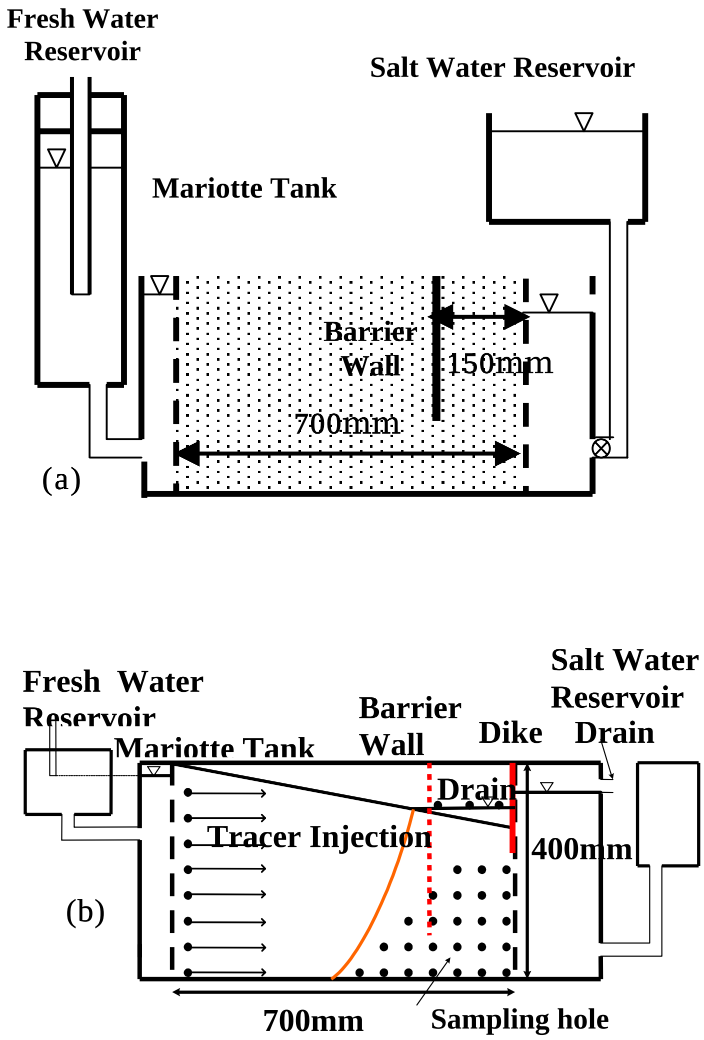

Fig. 1: Experimental apparatus for salt water intrusion in porous media with flat (a) and inclined (b) surfaces.

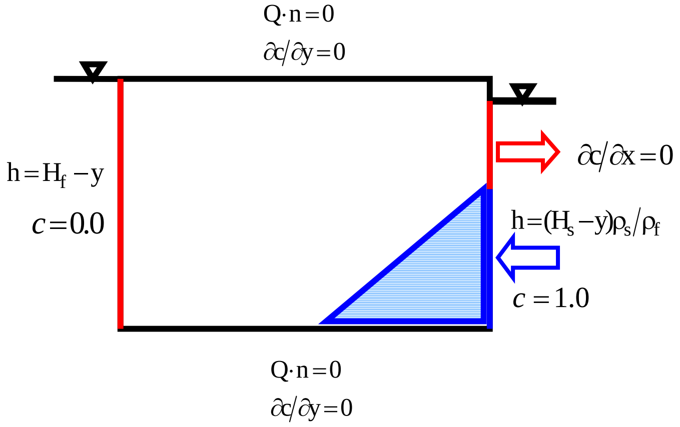

Fig. 2: Boundary conditions for fluid flow and mass transport equations.

MATHEMATICAL MODEL AND NUMERICAL SIMULATION

Within a non-deformable porous media, the governing equation for flow of non-compressive fluids with variable density is given by

$$\nabla \cdot \rho K_f \left(\nabla h_f + \frac{\rho}{\rho_f} \nabla z \right) = \frac{\partial \rho}{\partial t} \qquad (1)$$

where ρ, ρ_f are the density of fluid and fresh water, K_f, h_f are the hydraulic conductivity and the pressure head in terms of fresh water, and z is the upward vertical coordinate.

The governing equation for transport of conservative mass is given by

$$\nabla \cdot D \nabla C - \mathbf{v} \cdot \nabla C = \frac{\partial C}{\partial t} \qquad (2)$$

where D is the dispersion coefficient, C is the concentration of salt, and $\mathbf{v}$ is the fluid velocity vector.

Boundary conditions for Eq.(1) and Eq.(2) are given in Fig.2. Eq.(1) can be solved by the standard Galerkin finite element method, which procedure are referred in ordinary text books and omitted here.

According to Garder et al., Eq.(2) is equivalent to the following set of ordinary differential equations.

$$\frac{d\mathbf{x}}{dt} = \mathbf{v} \qquad (3)$$

$$\frac{dC}{dt} = \nabla \cdot (D \nabla C) \qquad (4)$$

Application of the Galerkin finite element method to Eq.(4) leads to

$$\left(\frac{[E]}{2} + \frac{[F]}{\Delta t} \right) \{ C(\mathbf{x}, t + \Delta t) \} = \left(\frac{[F]}{\Delta t} - \frac{[E]}{2} \right) \{ C(\mathbf{x} - \mathbf{v}\Delta t, t) \} \qquad (5)$$

where $C(\mathbf{x} - \mathbf{v}\Delta t, t)$ is the salt concentration of fluids at time t and at points where particles migrate along characteristic curves

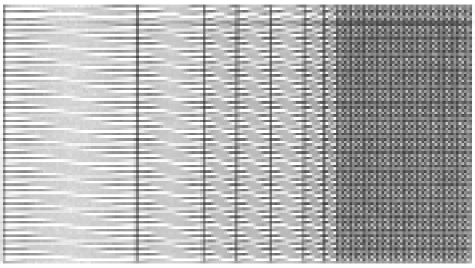

Fig. 3: Finite element mesh with 2160 elements and nodes of 1148 without to 1183 with barrier wall

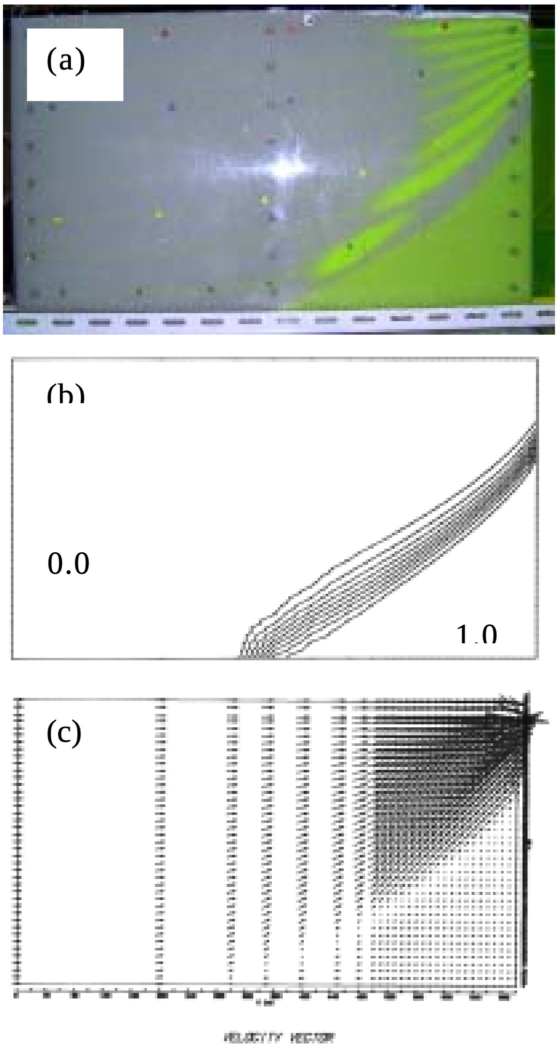

Fig. 4A: Experimental result (a) and calculated relative concentration distribution (b) and velocity vector distribution (c) for the case of flat surface without barrier wall.

onto each node during time interval Δt.

$$\left.\begin{aligned} E_{ij} &= \int_R D \frac{\partial \phi_i}{\partial x} \frac{\partial \phi_j}{\partial z} dR \\ F_{ij} &= \int_R \phi_i \phi_j dR \end{aligned}\right\} \quad i, j = 1,2,\cdots,N \qquad (6)$$

where ϕ is the shape function, R is the analytical domain and N is the number of nodes.

RESULTS

Fig.4A(a) shows an equilibrium-state experimental result of salt water intrusion for a case of flat surface without the barrier wall. Fresh water flows from left to right boundary monotonically. Fig.4B(a) for a case of flat surface with a barrier wall of 350 mm deep shows that fresh water flows downward along the wall and then upward to be discharged from the upper part of the right boundary. In both pictures, center of migrating tracer clouds were marked by dots to record stream lines. Comparison of both figures shows how the barrier wall works to prevent salt water intrusion.

Fig.5 shows salt water intrusion together with stream lines of fresh water for the experiment with inclined surface. When salt water level was low (Fig.5a), inundation was not severe compared with high salt water level (Fig.5b). In both cases fresh water seeped out along inclined surface, dived down along the dike foundation, and finally discharged to the right boundary. When the level of seeped-out water along inclined seepage face was lowered by drainage (Fig.5c), salt water intrusion was strongly enforced and salt water seeped out through the inclined surface. When a barrier wall of 250 mm deep was installed (Fig.5d), salt water intrusion was reduced but at the cost of inland inundation.

Some results of these experiments were simulated using the coupled analysis of variable-density flow by finite element method and mass transport by the aforementioned characteristic finite element method. (b) and (c) of Fig.4A and 4B are the calculated results of salt concentration distribution and the velocity vector distribution at stationary stage. Drastic changes in the direction of velocity vector near the toe of saltwater/ freshwater interface made the accurate tracking difficult and caused wide

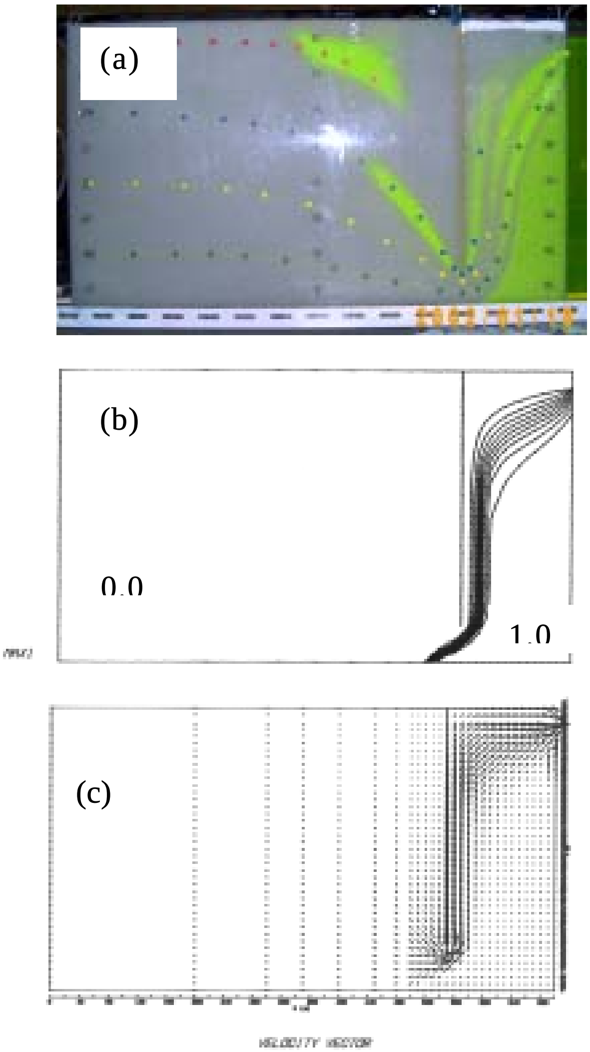

Fig. 4B: Experimental result (a) and calculate concentration distribution (b) and velocity vector distribution (c) for the case of flat surface with barrier wall.

ranges of transition zones compared with the experimental zones as pointed out by Benson et al. [1998].

.

CONCLUSIONS

Two types of laboratory experiments were carried out to investigate the impact of possible sea level rise on salt water intrusion into coastal aquifers. It is revealed from the experiments that reinforcement of dike's height may prevent storm surges but cannot prevent salt water intrusion and the following inundation in inland area. Drainage of excess inland water may further enhance salt water intrusion. Installation of barrier walls can prevent salt water intrusion to some extent at the cost of difficulties to drain excess inland water.

The best solution to stop possible hazardous events will be to reduce carbon dioxide drastically as soon as possible.

References

IPCC, *Technical Summary, Climate change, Impacts, adaptation, and vulnerability,* 2001.

Benson,D.A., Carey,A.E. and Wheatcraft,S.W., "Numerical advective flux in highly variable velocity fields exemplified by saltwater intrusion," *J. Contaminant Hydrology*, 34, 207-233, 1998.

Garder, A.O., Peaceman,D.W. and Pozzi,A.L.Jr., "Numerical calculation of multidimensional miscible displacement by the method of characteristics." J.Soc.Petrol.Engng., 4, 26-36, 1964.

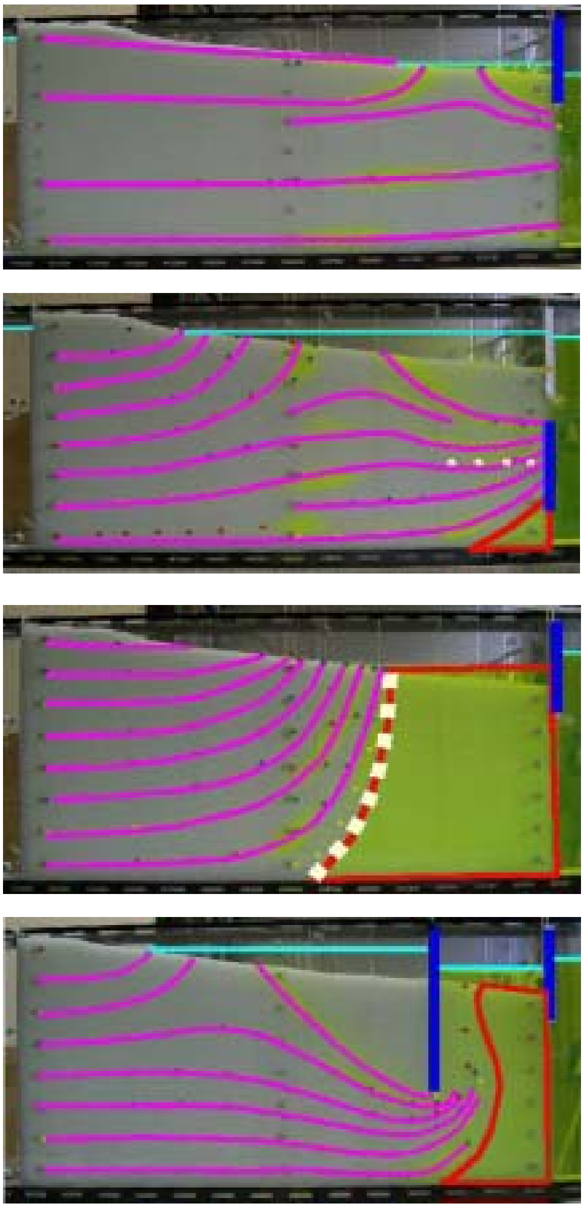

Fig. 5: Results of experimental with inclined surface for :(a) low salt water level, (b) high salt water level without inland drainage and barrier wall, (c) high salt water level with inland drainage and no barrier wall, (d) high salt water level with inland drainage and barrier wall.

Keywords: Sea level rise, laboratory experiment, barrier wall, numerical modeling

Corresponding author: Katsuyuki Fujinawa, Professor of Geo-Environmental Engineering, Faculty of Engineering, Shinshu University, Wakasato 4-17-1, Nagano, Japan 380-8553. Email: kfujina@gipwc.shinshu-u.ac.jp